SIMULTANEOUS DETECTION OF PROMINENT POINTS ON BREAST CANCER CONSERVATIVE TREATMENT IMAGES

Hélder P. Oliveira[1]*, Student Member, IEEE*
Jaime S. Cardoso[1]*, Senior Member, IEEE, André Magalhães*[2]*, Maria J. Cardoso*[3]

[1]INESC TEC (formerly INESC Porto) and Faculdade de Engenharia, Universidade do Porto
[2]Faculdade de Medicina, Universidade do Porto
[3]Champalimaud Cancer Center, Fundação Champalimaud

ABSTRACT

Breast Cancer Conservative Treatment (BCCT) is now the preferred technique for breast cancer treatment. The limited reproducibility of standard aesthetic evaluation methods led to the development of objective methods, such as Breast Cancer Conservative Treatment.cosmetic results (BCCT.core) software tool. Although the satisfying results, there are still limitations concerning complete automation and the inability to measure volumetric information.

With the fundamental premise of maintaining the system as a low-cost tool, the incorporation of the Microsoft Kinect sensor in BCCT evaluations was studied. The aim with this work is to enable the simultaneous detection of breast contour and breast peak points using depth-map data. Experimental results show that the proposed algorithm is accurate and robust for a wide number of patients. Additionally, comparatively to previous research, the procedure for detecting prominent points was automated.

***Index Terms*—** Biomedical image processing, medical information system, image analysis

1. INTRODUCTION

Breast-conserving therapeutic approaches to breast cancer aim to obtain, besides local tumour control and survival rates equivalent to mastectomy, better aesthetic results. While the oncological outcome of breast conservation procedures can easily be assessed objectively, the cosmetic outcome does not yet have an evaluation standard [1].

Initially, the aesthetic evaluation was performed by one or more observers either by directly observing the patient or photographs, using one of the existing scales that compare treated with non-treated breasts. The most widespread scale used for aesthetic evaluation of BCCT is the Harvard scale, introduced by Jay Harris in 1979. It classifies the overall cosmetic results in four classes from excellent, good, fair to poor. However, it soon became clear that this kind of subjective evaluation had important disadvantages. For instance, exemption is not guaranteed, reproducibility is difficult to achieve and the level of agreement between observers is low or moderate. Objective methods were introduced in an attempt to overcome the lack of objectivity and reproducibility. These methods consisted of comparing the two breasts with simple measurements marked directly on the patients or on photographs of them. However, initial methodologies continued to show a significant lack of standardization, not only in the type of assessment used, but also in the factors included in the evaluation and the instruments used. There was a need to replace or enhance the expert human evaluation with an objective, affordable, easy to use and highly reproducible validated tool.

BCCT.core [2] is a relatively recent computer-aided medical system and its aim is to overcome the disadvantages of previous methodologies. The development of BCCT.core consisted of semi-automatically extracting several features from frontal photographs of patients, capturing some of the factors which are considered to have an impact on the overall cosmetic results: breast asymmetry, skin colour changes caused by radiotherapy and surgical scar [2]. In a second phase, a Machine Learning algorithm is applied to predict the overall cosmetic result using the recorded features. Although innovative and reproducible, this tool has several points that need to be addressed. Some of these limitations have already been addressed, as is the case of the model's interpretability relating the aesthetic result with input measures [3]. However, there are important setbacks related to the complete automation of the software – which is fundamental for high reproducibility – and the capability to extract volumetric information to improve the overall cosmetic evaluation. Furthermore, the solutions should remain low-cost.

Several research groups have recently made attempts with 3D technology. These techniques are based on 3D cameras [4], 3D laser scanning or even optoelectronic tracking systems [5]. Current 3D technologies are very expensive and difficult to operate, thus requiring specialized staff. There-

The first author would like to thank Fundação para a Ciência e Tecnologia (FCT) - Portugal for the financial support for the PhD grant with reference SFRH/BD/43772/2008. This work was also partially funded by FCT - Portugal through project PTDC/SAU-ENB/114951/2009.

fore, this is not a feasible option for daily clinical practice and its widespread use in the near future is not foreseeable. Almost all techniques based on 3D models used nowadays do not try to predict the aesthetic result for an informed choice of treatment, nor are they suitable to automatically evaluate aesthetic results after surgery. Moreover, 3D reconstruction of breasts is a very difficult task since it is featureless.

We have recently introduced Microsoft Kinect [6] as a promising low-cost and easy to use equipment for BCCT cosmetic evaluation, because it can not only facilitate automation, but also provide volumetric information. In this paper, the simultaneous extraction of breast contour and breast peak points is addressed, using the depth-map image resulting from the acquisition performed by the Kinect sensor (see Fig. 2(d)).

In [7] authors introduced a semi-automatic method to detect the breast contour in frontal colour images. The contour is found based on previously known start and end points. Subsequently, the algorithm automatically finds the contour in-between using graph theory. As a result, the algorithm finds the minimum cost path between previously known end points provided manually by the user. This line of work was improved in [8], where both the start and end points are found automatically. External points of the contour are detected, considered the area of the body where the arm contour intersects the trunk contour. However, and depending on the patient's arm position, the contour of the arm and trunk can be overlapped, and thus it can be impossible to distinguish when patients put their upper limbs down. This problem is overcome by searching for the strongest vertical gradient lines. However, this does not work if patients assume different arm positions. Other authors are still using manually delineated breast contours and fiducial points [9].

2. SIMULTANEOUS DETECTION OF BREAST CONTOUR AND BREAST PEAK POINTS

Researchers are now paying more attention to the context to aid visual recognition processes. Context plays an important role in the human visual system's recognition processes and many important visual recognition tasks critically rely on context. The goal of this paper is to model the mutual context of *breast contour* and *breast peak* (the area in the breast closer to the camera or further away from the chest wall, not necessarily the nipple) so that each can facilitate the recognition of the other. When performed independently, both tasks are non-trivial since many other parts of the image may be falsely detected. However, the two tasks can benefit greatly from serving as context for each other. To model the breast peak point, a filter is used which evaluates the degree of divergence of the gradient vectors within its region of support from a pixel of interest. The breast contour is modelled as a short path in a graph whose nodes correspond to the pixels in the image and the edges connect neighbouring pixels. The weight function on the edges is defined so that short paths correspond to paths that maximize the amount of gradient strength in the image along the path. The quality or probability of the join model for the co-occurrence of breast peak and breast contour will be proportional to the individual qualities of the two parts. Next, the proposed algorithm is described in detail.

2.1. Proposed Algorithm

The proposed algorithm can be implemented as a sequence of a few high-level operations, as presented in Fig. 1.

Fig. 1. Algorithm flowchart.

Two simplifications are adopted in relation to the main rationale outlined above. Firstly, the detection will be performed over the patient's body only to speed up the computation. Secondly, the simultaneously detection of the peak and breast contour will be addressed first by over-detecting peak candidates, followed by a contour detection near them.

Similarly to other depth measuring technologies, such as laser scanners or range finding cameras, the output of the Kinect contains a large amount of missing data and noise, as a result of occlusions. Typically represented as white pixels, these missing values are excluded from all of the following operations. All the remaining pixels were scaled between 0 and 1. Finally, a 3×3 smooth filter was applied to eliminate noise resulting from acquisition. Fig. 2(c) and Fig. 2(d) already shows the output of this pre-processing task.

2.1.1. Adaptive background segmentation

Although the background should preferably be uniform for the acquisition process, the background is often cluttered. The presence of different objects at different depths, possibly at depths similar to the patient's, or just the different body parts at different depths, dismisses the application of simple thresholding methods as Otsu's (see Fig. 2(c)). Here, a situation is explored where the patient is at a somewhat central position in the image and is likely the 'object' closer to the camera.

In order to exploit this property, a density image is defined by transforming the depth information on the XY plane to the XZ plane [10]. The value at position (x, z) of the density image denotes the number of points in the depth image at position x (histogram of the column x), taking the value z (by counting along the Y direction), (see Fig. 2(a)). Then for each (x, z) position we computed the variance above and below. Each column x presents 3 different patterns: (1) background; (2)'object' and background; (3) 'object'. The XZ image is then replaced by the following rule: (1) cumulative value of the minimum of the variance from 1 to $Nbins$; (2) average of the two variances; (3) cumulative value of the minimum of the variance from $Nbins$ to 1 (see Fig. 2(b))

A global thresholding method of the original XY image corresponds to defining a horizontal line in the XZ image, discriminating background from foreground (see Fig. 2(a) and Fig. 2(c)). An adaptive thresholding method can be defined as a curve in the XZ image from left to right margins. This results in a threshold that varies from column to column in the original XY image. Since it is necessary for the curve in the XZ image to avoid the parts of the image with high values (high countings), the threshold curve was computed as the shortest path from left to right margin, where the cost of each pixel is its 'intensity' value (see Fig. 2(b) and Fig. 2(d)).

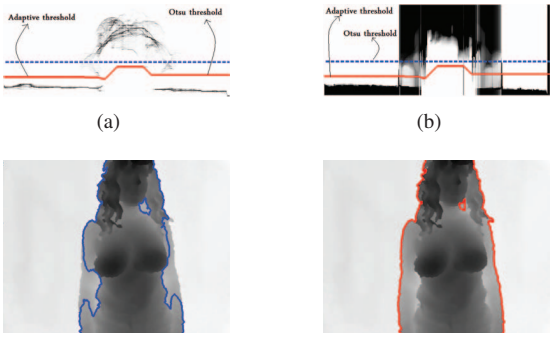

(a) (b)

(c) (d)

Fig. 2. a) XZ plane depth information; b) XY variance plane; c) Otsu's segmentation; d) Adaptive segmentation.

2.1.2. Convergence filter and fiducial points selection

A major benefit of using depth-map images has to do with high contrasts in the breast area. The peak point of the breast corresponds to the point in the breast where disparity attains the lowest value. The typically round or tear drop shape of a breast leads to a distinctive pattern in the gradient vector field where the gradient diverge in all directions (see Fig. 3(a)).

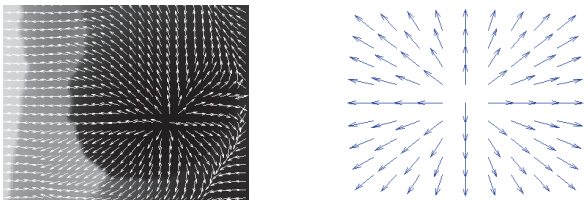

(a) (b)

Fig. 3. (a) Breast gradient vector field (5-pixel spacing); (b) Template vector field

In order to detect peaks in the breast, an approach similar to the Convergence Index Filter [11] was used in which the image was filtered with a radial vector field pattern, as presented in Fig. 3(b). Only the gradient orientation angle was used in the matching process, by previously normalizing the norm of the gradient vectors to unity. The similarity between the template and the image was assessed using two different measures: cross-correlation $((f * g)[n] \stackrel{def}{=} \sum f^*[m]g[n+m])$, where f^* denotes the complex conjugate of f; and circular correlation introduced by Nicholas Fisher in 1983. Breast peak candidates correspond to all local maximum positions.

2.1.3. Contour detection

Breast contour detection was performed using a shortest-path approach similarly to [8]. Intuitively, breast boundary manifests itself as a change in the grey-level values of the pixels, thus originating to an edge in the resulting image. Therefore, interpreting the image as a graph with each pixel as a node and edges connecting adjacent pixels, the breast contour corresponds to a low-cost path through edge pixels, with the appropriate weight function. Since the breast contour is approximately circular and centered on the breast peak candidates, the computation is more naturally performed by adopting polar coordinates, with the origin of the coordinates in the peak candidate. Each column in the polar image corresponds to the gradient along each radial line in the original space, computed using a 3-point numerical differentiation: $G_\theta(r) = \frac{f(r+h)-f(r-h)}{2h}$, where $h = 1$ and r is the radius. Then, the gradient image is considered as a weighted graph with pixels as nodes and edges connecting neighbouring pixels. Each 4-neighbour pixel arc corresponds to a weight determined by the gradient value of the two incident pixels, expressed as an exponential law: $f(g) = f_l + (f_h - f_l)\frac{exp(\beta(255-g))-1}{\exp(\beta 255)-1}$, with $f_l, f_h, \beta \in \Re$ and g is the minimum of the gradient computed on the two incident pixels. For 8-neighbour pixels the weight was set to $\sqrt{2}$ times that value. The parameters f_l, f_h, and β were fixed at $f_l = 2$, $f_h = 128$, $\beta = 0.0208$.

In this work, we are mainly interested in obtained the localization of the breast contour, not so much in its complete delineation. Therefore, the angle θ was varied only between π and 2π (see Fig. 4(a)). The candidate contour was then the output of the shortest path algorithm in the polar image (see Fig. 4(b)). The shortest path was computed between the whole external margin and a single point (point of highest gradient) in the internal margin.

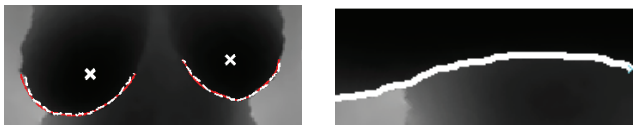

(a) (b)

Fig. 4. (a) Breast contour - ground truth (solid red line), detected (dashed white line); (b) Polar image and detected contour (white line).

2.1.4. Breast peak points and breast contour decision

The join decision for breast peak point and contour is taken to maximize the join probability of the individual parts. In here, we assume that the join probability is a monotonous function of the product of the correlation outputted by the divergence

filter and the quality of the detected contour. The quality of the contour is evaluated by the average magnitude of the gradient along it. Therefore, the final decision consists in selecting the pair (peak, contour) that maximizes the quality measure. Taking advantage of the body symmetry with respect to the sagittal plane, a pair (peak, contour) was selected to the right and another pair to the left of the body centre of mass.

3. RESULTS

The database now consists of 144 cases acquired during several sessions throughout an entire year. For each patient the acquired data include the depth-map image and the colour image acquired with Kinect (640×480 px) and a colour image acquired with a standard 5MP portable camera. Only Kinect depth-map image is used in this work. Manual ground truth annotation was performed both to breast peaks position and breast contour definition.

The breast peak points detection accuracy was measure using Euclidean metric distance (see Table 1).

Table 1. Breast peak points detection error (in pixels).

Metric	Breast	Standalone		Simultaneous detection	
		μ (σ)	# Miss	μ (σ)	# Miss
Circ. corr.	Right	18.02 (46.86)	16	8.23 (14.34)	8
	Left	13.61 (39.02)		10.32 (27.51)	
Cross-corr.	Right	8.65 (17.65)	4	5.81 (3.44)	0
	Left	6.68 (3.60)		6.68 (3.60)	

First column (standalone) shows the detection error that would be obtained by grounding the decision on the maximization of the output of the convergence filter. The second column (simultaneous detection) depicted the performance for the proposed scheme. Miss detection means that breast peak point was detected outside from breast area. It is clear the advantage of the proposed method. Moreover the cross-correlation attains better results both in the mean error and in the miss detection.

Breast contour detection error using the join model for the co-occurrence of breast peak and breast contour was evaluated based on the Hausdorff and the average distances (Table 2). The Hausdorff distance is defined as $h(A,B) = \max_{a \in A} \min_{b \in B} \|a - b\|$, where B represents the set of pixels of the ground truth and A the segmented breast contour; $\|.\|$ is the Euclidean distance. The motivation for using this metric is that is represents the worst case scenario.

Table 2. Breast contour detection error (in pixels).

	Right breast		Left breast	
	Mean	Hausdorff	Mean	Hausdorff
Average	1.80	4.88	1.83	5.21
Stdev	0.90	2.27	1.11	2.80
Max	6.55	14.72	5.90	15.95
Min	0.71	2.20	0.63	1.89

Since the Kinect resolution is 1.3mm/px, the average error corresponds to 2.36mm, a better result than obtained in previous work [7] using frontal patient colour images.

4. CONCLUSIONS

In this paper we present the simultaneous detection of prominent points in breast using depth-map data acquired with Microsoft Kinect sensor. Breast peak points were found based on gradient vector field information associated with convergence filter theory. Breast contour was found as the solution to the shortest-path problem is the graph theory framework, after conveniently modelling the image as a weighted graph. It was shown that depth-map images facilitate the automation of BCCT.core, maintaining this software as low-cost and easy to perform. Obtained results also indicate an excellent performance and robustness for a wide variety of patients. Future work will focus on the detection of the complete breast contour, including start and end points, conversion of prominent points to colour images and extraction of volumetric information.

5. REFERENCES

[1] M. J. Cardoso, J. S. Cardoso, C. Vrieling, D. Macmillan, D. Rainsbury, J. Heil, E. Hau, and M. Keshtgar, "Recommendations for the aesthetic evaluation of breast cancer conservative treatment (submitted)," *Breast Cancer Research and Treatment*, 2012.

[2] J. S. Cardoso and M. J. Cardoso, "Towards an intelligent medical system for the aesthetic evaluation of breast cancer conservative treatment," *Artificial Intelligence in Medicine*, vol. 40, pp. 115–126, 2007.

[3] H. P. Oliveira, A. Magalhaes, M. J. Cardoso, and J. S. Cardoso, "An accurate and interpretable model for bcct.core," in *Proceedings of the 32nd Annual International Conference of the IEEE Engineering in Medicine and Biology Society*, 2010, pp. 6158 – 6161.

[4] H. R. Moyer, G. W. Carlson, T. M. Styblo, and A. Losken, "Three-dimensional digital evaluation of breast symmetry after breast conservation therapy," *Journal of the American College of Surgeons*, vol. 207, no. 2, pp. 227 – 232, 2008.

[5] G. Catanuto, P. Patete, A. Spano, A. Pennati, G. Baroni, and M. B. Nava, "New technologies for the assessment of breast surgical outcomes," *Aesthetic Surgery Journal*, vol. 29, no. 6, pp. 505 – 508, 2009.

[6] H. P. Oliveira, P. Patete, G. Baroni, and J. S. Cardoso, "Development of a bcct quantitative 3d evaluation system through low-cost solutions," in *Proceedings of the 2nd International Conference on 3D Body Scanning Technologies*, 2011, pp. 16–27.

[7] R. Sousa, J. S. Cardoso, J. F. Pinto da Costa, and M. J. Cardoso, "Breast contour detection with shape priors," in *Proceedings of the 15th IEEE International Conference on Image Processing*, 2008, pp. 1440–1443.

[8] J. S. Cardoso, L. F. Teixeira, and M. J. Cardoso, "Automatic breast contour detection in digital photographs," in *Proceedings of the International Conference on Health Informatics*, 2008, vol. 2, pp. 91–98.

[9] J. Lee, E. K. Beahm, M. A. Crosby, G. P. Reece, and M. K. Markey, "Analysis of breast contour using rotated catenary," in *AMIA Annual Symposium Proceedings*, 2010, pp. 432–436.

[10] N. F. Kim and J. S. Park, "Segmentation of object regions using depth information," in *Proceedings of the International Conference on Image Processing*, 2004, pp. 231–234.

[11] H. Kobatake and S. Hashimoto, "Convergence index filter for vector fields," *IEEE Transactions on Image Processing*, vol. 8, no. 8, pp. 1029 –1038, 1999.